

# MatchFormer: Interleaving Attention in Transformers for Feature Matching

Qing Wang\*, Jiaming Zhang\*, Kailun Yang<sup>†</sup>, Kunyu Peng, Rainer Stiefelhagen  
CV:HCI Lab, Karlsruhe Institute of Technology, Germany

## Abstract

Local feature matching is a computationally intensive task at the subpixel level. While detector-based methods coupled with feature descriptors struggle in low-texture scenes, CNN-based methods with a sequential extract-to-match pipeline, fail to make use of the matching capacity of the encoder and tend to overburden the decoder for matching. In contrast, we propose a novel hierarchical extract-and-match transformer, termed as MatchFormer. Inside each stage of the hierarchical encoder, we interleave self-attention for feature extraction and cross-attention for feature matching, enabling a human-intuitive extract-and-match scheme. Such a match-aware encoder releases the overloaded decoder and makes the model highly efficient. Further, combining self- and cross-attention on multi-scale features in a hierarchical architecture improves matching robustness, particularly in low-texture indoor scenes or with less outdoor training data. Thanks to such a strategy, MatchFormer is a multi-win solution in efficiency, robustness, and precision. Compared to the previous best method in indoor pose estimation, our lite MatchFormer has only 45% GFLOPs, yet achieves a +1.3% precision gain and a 41% running speed boost. The large MatchFormer reaches state-of-the-art on four different benchmarks, including indoor pose estimation (ScanNet), outdoor pose estimation (MegaDepth), homography estimation and image matching (HPatch), and visual localization (InLoc).<sup>1</sup>

## 1. Introduction

Matching two or more views of a scene is the core of many basic computer vision tasks, e.g., Structure-from-Motion (SfM) [19, 31], Simultaneous Localization and Mapping (SLAM) [4, 11], relative pose estimation [16], and visual localization [29, 34, 44], etc. For vision-based matching, classical *detector-based* methods (see Fig. 2(a)), coupled with hand-crafted local features [10, 28], are computationally intensive due to the high dimensionality of lo-

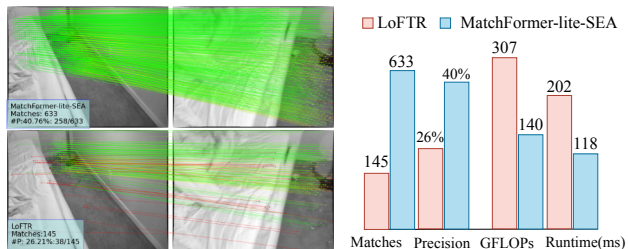


Figure 1. **Comparison between MatchFormer and LoFTR.** With 45% GFLOPs of LoFTR, our efficient MatchFormer boosts the running speed by 41%, while delivering more robust matches and a higher matching precision on such a low-texture indoor scenario. Green color in the figure refers to correct matches and red color to mismatches.

cal features [29, 53]. Recent works [22, 26, 40] based on deep learning focus on learning detectors and local descriptors using Convolutional Neural Networks (CNNs). However, CNNs experience difficulties capturing global expressions, e.g., long-distance relationships among visual elements [53]. Finding correspondences in texture-less scenes is based not only on local neighborhoods, but also on a wider global context [33]. For example, the low-texture regions in images look locally similar but can be distinguished by long-range and context-relevant textured elements (e.g., edges and corners). Thus, extracting fine local features and learning the long-distance relationship between visual elements are both indispensable [30, 33].

Recently, the transformer architecture [38] has been introduced to many visual tasks [3, 9, 50], which can capture complex spatial transformations and long-distance feature dependencies, forming a global representation conducive to feature matching in texture-sparse scenes. Yet, one should be noted that higher resolution is better for local feature matching [33]. Unfortunately, the computation of the self-attention is expensive for high-resolution inputs [39]. However, some partial transformer-based methods [14, 33] only design an attention-based decoder and remain the *extract-to-match* pipeline (see Fig. 2(b)). For instance, while COTR [14] feeds CNN-extracted features into a transformer-based decoder, SuperGlue [30] and LoFTR [33] only apply attention modules atop the decoder.

\*Equal contribution

<sup>†</sup>Correspondence: kailun.yang@kit.edu

<sup>1</sup>Code will be made publicly available at [MatchFormer](#).

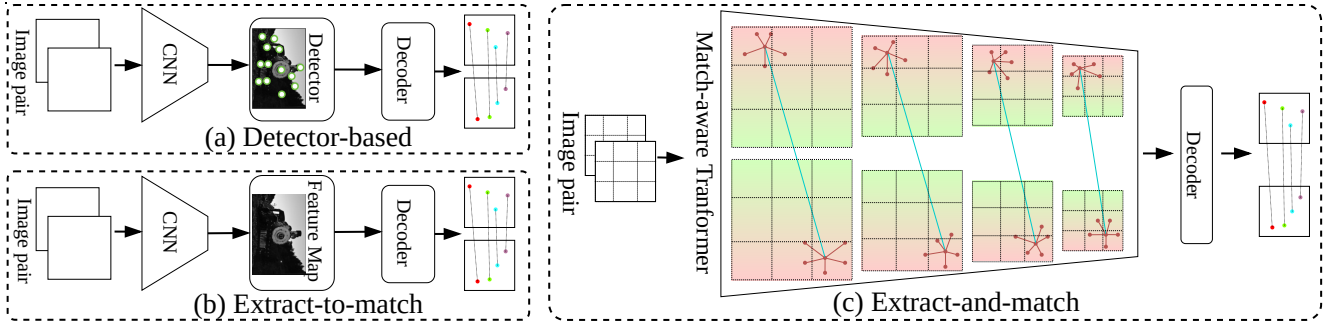


Figure 2. **Different matching pipelines.** Self- and cross-attention are interleaved inside each stage of the match-aware transformer to perform an extract-and-match pipeline.

Overburdening the decoder, yet neglecting the matching capacity of the encoder, makes the whole model computationally inefficient.

Rethinking local feature matching, in reality, one can perform feature extraction and matching simultaneously by using a pure transformer, i.e., an *extract-and-match* pipeline (see Fig. 2(c)). Compared to the *detector-based* methods and the *extract-to-match* pipeline, our new scheme is more in line with human intuition, which learns more respective features of image pairs while paying attention to their similarities [51]. To this end, a novel pure transformer termed *MatchFormer* is proposed, which helps to achieve multi-wins in precision, efficiency, and robustness of feature matching, as compared with LoFTR [33] in Fig. 1.

More specifically, for improving computational efficiency and the robustness in matching low-texture scenes, we put forward *interleaving* self- and cross-attention in MatchFormer to build a matching-aware encoder. In this way, the local features of the image itself and the similarities of its paired images can be learned simultaneously, so called *extract-and-match*, which relieves the overweight decoder and makes the whole model efficient. The cross-attention arranged in earlier stages of the encoder robustifies feature matching, particularly, in low-texture indoor scenarios or with less training samples outdoors, which makes MatchFormer more suitable for real-world applications where large-scale data collection and annotation are infeasible. To extract continuous patch information and embed location information, a novel *positional patch embedding* (*PosPE*) method is designed in the matching-aware encoder, which can enhance the detection of low-level features. Additionally, the lite and large versions *w.r.t.* feature resolutions, each with two efficient attention modules [32, 41], are fully investigated to overcome the massive calculations in transformers when dealing with fine features. Furthermore, MatchFormer, with a hierarchical transformer, conducts multi-level feature extraction in the encoder and multi-scale feature fusion in the decoder, which contribute to the robustness of matching. Finally, for the

precision, extensive experiments prove that MatchFormer achieves state-of-the-art performances of indoor location estimation on ScanNet [7], outdoor location estimation on MegaDepth [18], image matching and homography estimation on HPatches [1], and visual localization on InLoc [34].

In summary, the contributions of this paper include:

- We rethink local feature matching and propose a new *extract-and-match* pipeline, which enables synchronization of feature extraction and feature matching. The optimal combination path is delivered when *interleaving* self- and cross-attention modules within each stage of the hierarchical structure to enhance multi-scale features.
- We propose a novel vision transformer, i.e., *MatchFormer*, equipped with a robust hierarchical transformer encoder and a lightweight decoder. Including lite and large versions and two attention modules, four variants of MatchFormer are investigated.
- We introduce a simple and effective positional patch embedding method, i.e., *PosPE*, which can extract continuous patch information and embed location information, as well as enhances the detection of low level features.
- MatchFormer achieves state-of-the-art scores on matching low-texture indoor images and is superior to previous *detector-based* and *extract-to-match* methods in pose estimation, homography estimation, and visual localization.

## 2. Related Work

**Local Feature Matching.** *Detector-based* methods [6, 10, 13, 23] usually include five steps: detecting interest points, calculating visual descriptors, searching for nearest neighbor matches, rejecting incorrect matches, and estimating geometric transformations. In *extract-to-match* methods [10, 17, 26, 30, 33, 36] designed for feature matching, CNNs are normally adopted to learn dense and discriminative features. CAPS [40] fuses multi-resolution features extracted by CNNs and obtains the descriptor of

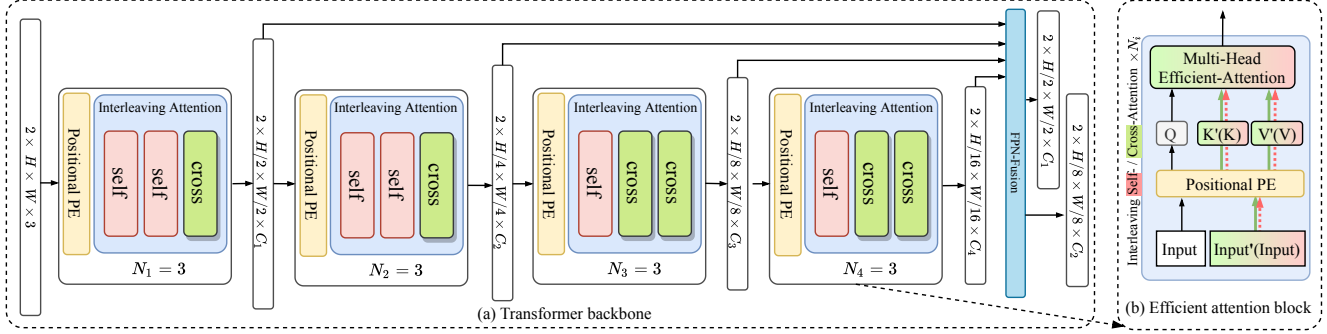


Figure 3. **MatchFormer architecture:** (a) The transformer backbone generates high-resolution coarse features and low-resolution fine features; In (b), each attention block has interleaving-arranged self-attention (*w.r.t.*  $Q, K, V$  and red arrows) within the *input*, and cross-attention (*w.r.t.*  $Q, K', V'$  and alternative green arrows) cross images (*input* and *input'*). Multi-head efficient-attention reduces the computation; Positional Patch Embedding (PE) completes the patch embedding and the position encoding.

each pixel through interpolation. DSM [35] strengthens detection and refines the descriptors by merging various frames and multiple scales extracted by CNNs. DRC-Net [17] obtains CNN feature maps of two different resolutions, generates two 4D matching tensors, and fuses them to achieve high-confidence feature matching. D2Net [10] obtains valid key points by detecting the local maximum of CNN features. R2D2 [26] adapts dilated convolutions [5, 45] to maintain image resolution and predict each key points and descriptors. COTR [14], LoFTR [33], and QuadTree [36] follow sequential *extract-to-match* processing. In this work, we consider that feature extraction and similarity learning through a transformer synchronously, can provide matching-aware features in each stage of the hierarchical structure.

**Vision Transformer.** Transformer [9] excels at capturing long-distance dependency [38], making it outstanding in vision tasks such as classification [20, 37, 46], detection [3, 41, 54], semantic segmentation [42, 48, 50], image enhancement [49], and image synthesis [12]. For local-feature matching, only attention blocks of transformers have been used in recent works. For example, SuperGlue [30] and LoFTR [33] applied self- and cross-attention to process the features which were extracted from CNNs. Yet, attention can actually function as the backbone module for feature extraction instead of only being used in the decoder for CNNs. This has been verified in ViT [9], but mainly for classification and segmentation tasks [41, 50]. It remains unclear whether it is transferable to the image feature matching. When a pure transformer framework is used to process local feature matching, the computation complexity will be exceedingly large. Besides, transformers often lack and miss local feature information [46]. In this paper, we put forward a fully transformer image matching framework. In our model, we design positional patch embedding to enhance the feature extraction and introduce interleaving attention to achieve efficient and robust feature matching.

## 3. Methodology

### 3.1. MatchFormer

As illustrated in Fig. 3, MatchFormer employs a hierarchical transformer, which comprises four stages to generate high-resolution coarse and low-resolution fine features for local feature matching. In four stages, the self- and cross-attention are arranged in an *interleaving* strategy. Each stage consists of two components: one *positional patch embedding* (*PosPE*) module, and a set of efficient attention modules. Then, the multi-scale features are fused by an FPN-like decoder. Finally, the coarse and fine features are passed to perform the coarse-to-fine matching, as introduced in LoFTR [33].

**Interleaving Self-/Cross-Attention.** As shown in Fig. 3(a), the combination of self- and cross-attention modules are set at each stage in an *interleaving* strategy. Each block in Fig. 3(b) contains  $N$  attention modules, where each attention module is represented as self-attention or alternative cross-attention according to the input image pair. For self-attention,  $Q$  and  $(K, V)$  come from the same *input*, so the self-attention is responsible for feature extraction of the image itself. For cross-attention,  $(K', V')$  are from another *input'* of the image pair. Thus, the cross-attention learns the similarity of the image pair. Unlike the *extract-to-match* LoFTR using attention on a single-scale feature map and only after feature extraction, we interleave self- and cross-attention inside the encoder and on multiple feature scales. The interleaving strategy is able to learn features and explore their similarities simultaneously, *i.e.*, the *extract-and-match* scheme. As the feature map of the shallow stage emphasizes textural information, more self-attention are applied to focus on exploring the feature itself on the early stages of MatchFormer. The feature map at the deep stage is biased toward semantic information. Thus, developing more cross-attention to explore similarity is more efficient. Within an attention block, self-attended features are ex-

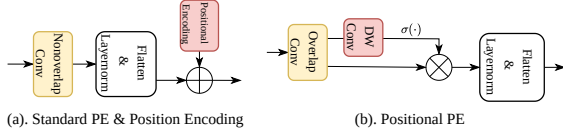


Figure 4. Comparison between different patch embedding modules.

tracted, while the similarity of the feature pair is located by the cross-attention. The strategy is more human-intuitive, which learns more respective features of image pairs while paying attention to their similarities.

**Positional Patch Embedding (PosPE).** Typical transformers [9], split the image ( $H \times W \times 3$ ) into patches with size of  $P \times P$  and then flatten these patches into sequence with a size of  $N \times C$ , where  $N = HW/P^2$ . The process is difficult to gather location information around patches. As a result, low-level feature information cannot be acquired directly through the standard process [46], which severely restricts the local feature matching. In the case of standard Patch Embedding (PE) in Fig. 4(a), the independent patch ignores the information around it and requires additional position encoding at the end. Therefore, we propose a simple but effective positional patch embedding (PosPE) method for capturing low feature information with few parameters, as shown in Fig. 4(b). It has a  $7 \times 7$  convolution layer (with padding 3 and stride 2) in the first stage, and  $3 \times 3$  convolution layers (all with padding 1 and stride 2) in later stages. A depth-wise  $3 \times 3$  convolution is added to further enhance local features and encode positional information by its padding operation. The pixel-wise weights are then scaled by a sigmoid function  $\sigma(\cdot)$  after the first step of convolution. Besides, our PosPE includes a first overlapping convolution that captures the continuous patch area information. PosPE augments the location information of patches and extracts denser features, which facilitates accurate feature matching.

**Efficient-Attention.** After Patch Embedding, the query  $Q$ , key  $K$ , and value  $V$  are obtained, with the same  $N \times C$  dimension according to the input resolution  $N = H \times W$ . The computation of the traditional attention is formulated as:  $\text{softmax}((QK^T)/\sqrt{d})V$ , where  $\sqrt{d}$  is the scaling factor. However, the product of  $QK^T$  introduces a  $O(N^2)$  complexity, which is prohibitive in large image resolutions and makes the model inefficient. To remedy this problem, we adapt to use two kinds of efficient attention, *i.e.*, *Spatial Efficient Attention (SEA)* as in [41, 42] or *Linear Attention (LA)* as in [32]. Then,  $O(N^2)$  is reduced to  $O(N^2/R)$  or  $O(N)$ . Hence, larger input feature maps can be well handled and processed while using a pure transformer-based encoder in the feature matching task.

SEA reduces the spatial scale of  $K$  and  $V$ . For brevity, SEA as self-attention is described as:  $\text{softmax}((Q \cdot SE(K^T)/\sqrt{d}) \cdot SE(V))$ , where  $SE(\cdot)$  refers to first reshaping the sequence  $N \times C$  to  $\frac{N}{R} \times (C \times R)$

and then projecting the dimension ( $C \times R$ ) to  $C$ . The complexity of the attention module is reduced from  $O(N^2)$  to  $O(N^2/R)$ , where  $R$  denotes the down-scale ratio.

LA reduces the complexity by replacing the exponential kernel of the original attention layer with a kernel function  $\text{sim}(Q; K) = f(Q) \cdot f(K)^T$ ,  $f(\cdot) = \text{elu}(\cdot) + 1$ . Utilizing the associativity property of matrix products, the multiplication between  $K$  and  $V$  can be carried out first. Due to  $D \times N$  ( $D \ll N$ ), the complexity is reduced from  $O(N^2)$  to  $O(N)$ .

**Multi-scale Feature Fusion.** Apart from the interleaving combination, there are four different stages in our hierarchical transformer encoder, in which the feature resolution shrinks progressively. Different from previous works [14, 17] considering only the single-scale feature, MatchFormer fuses multi-scale features to generate dense and match-aware features for feature matching. As shown in Fig. 3(a), we flexibly adopt an FPN-like decoder in our architecture, because it can bring two benefits: (1) generating more robust coarse- and fine features for promoting the final matching; (2) creating a lightweight decoder without making the whole model computationally complex.

## 4. Experiments

### 4.1. Settings and Datasets

**MatchFormer Variants.** MatchFormer is available with its lite and large versions, where the details of the variants of MatchFormer are presented in Table 1. For the MatchFormer-lite models, we pick a lower resolution setting, which greatly increases the matching efficiency and ensures a certain matching accuracy. Therefore, we set MatchFormer-lite 4-stage features in the respective resolution of  $\frac{1}{r_i} \in \{\frac{1}{4}, \frac{1}{8}, \frac{1}{16}, \frac{1}{32}\}$  of the input. To promote context learning for matching, feature embeddings with higher channel numbers are beneficial, which are set as  $C_i \in \{128, 192, 256, 512\}$  for four stages. In the MatchFormer-large models, higher resolution feature maps facilitate accurate dense matching. Hence, the  $\frac{1}{r_i}$  and  $C_i$  are set as  $\{\frac{1}{2}, \frac{1}{4}, \frac{1}{8}, \frac{1}{16}\}$  and  $\{128, 192, 256, 512\}$  for the large MatchFormer.

**Attention Module Variants.** Each of the two MatchFormer variants has two attention variants, which are Linear Attention (LA) and Spatial Efficient Attention (SEA). Thus, there are four versions of MatchFormer as presented in Table 1. We found that they have different capabilities for recognizing features, making them suitable for various tasks. In the local feature matching, the density of features is different indoors and outdoors. We study the two kinds of attention in indoor (in Sec. 4.2) and outdoor (in Sec. 4.3) pose estimation, respectively.

**ScanNet.** We use ScanNet [7] to train our indoor models. ScanNet is an indoor RGB-D video dataset with 2.5 million



Stage	MatchFormer-lite		MatchFormer-large		$N_i$
$F_1$	$H/4 \times W/4$	$K=7, S=4, P=3, E=4$	$H/2 \times W/2$	$K=7, S=2, P=3, E=4$	$\times 3$
	$C_1=128$	<b>LA:</b> $A=8$ ; <b>SEA:</b> $A=1, R=4$	$C_1=128$	<b>LA:</b> $A=8$ ; <b>SEA:</b> $A=1, R=4$	
$F_2$	$H/8 \times W/8$	$K=3, S=2, P=1, E=4$	$H/4 \times W/4$	$K=3, S=2, P=1, E=4$	$\times 3$
	$C_2=192$	<b>LA:</b> $A=8$ ; <b>SEA:</b> $A=2, R=2$	$C_2=192$	<b>LA:</b> $A=8$ ; <b>SEA:</b> $A=2, R=2$	
$F_3$	$H/16 \times W/16$	$K=3, S=2, P=1, E=4$	$H/8 \times W/8$	$K=3, S=2, P=1, E=4$	$\times 3$
	$C_3=256$	<b>LA:</b> $A=8$ ; <b>SEA:</b> $A=4, R=2$	$C_3=256$	<b>LA:</b> $A=8$ ; <b>SEA:</b> $A=4, R=2$	
$F_4$	$H/32 \times W/32$	$K=3, S=2, P=1, E=4$	$H/16 \times W/16$	$K=3, S=2, P=1, E=4$	$\times 3$
	$C_4=512$	<b>LA:</b> $A=8$ ; <b>SEA:</b> $A=8, R=1$	$C_4=512$	<b>LA:</b> $A=8$ ; <b>SEA:</b> $A=8, R=1$	
<b>Output</b>	Coarse: $H/4 \times W/4, 128$ Fine: $H/8 \times W/8, 192$		Coarse: $H/2 \times W/2, 128$ Fine: $H/8 \times W/8, 256$		

Table 1. **MatchFormer-lite and -large with Linear Attention (LA) and Spatial Efficient Attention (SEA).**  $C$ : the channel number of feature  $F$ ;  $K$ ,  $S$  and  $P$ : the patch size, stride, and padding size of PosPE;  $E$ : the expansion ratio of MLP in an attention block;  $A$ : the head number of attention;  $R$ : the down-scale ratio of SEA.

views in 1,513 scans with ground-truth poses and depth maps. The lack of textures, the ubiquitous self-similarity, and the considerable changes in viewpoint make ScanNet a challenging dataset for indoor image matching. Following [30], we select 230 million image pairs with the size of  $640 \times 480$  as the training set and 1,500 pairs as the testing set.

**MegaDepth.** Following [10], we use MegaDepth [18] to train our outdoor models, which has 1 million internet images of 196 scenarios, and their sparse 3D point clouds are created by COLMAP [31]. We use 38,300 image pairs from 368 scenarios for training, and the same 1,500 testing pairs from [33] for evaluation.

**Implementation Settings.** On the indoor dataset ScanNet, MatchFormer is trained using Adam [15] with initial learning rate and batch size, setting for the lite version at  $3 \times 10^{-3}$  and 4, and for the large version at  $3 \times 10^{-4}$  and 2. In the case of the outdoor dataset MegaDepth, MatchFormer is trained using Adam [15] with initial learning rate and batch size, setting for the lite version at  $3 \times 10^{-3}$  and 2, and for the large version at  $3 \times 10^{-4}$  and 1. All models are trained on 64 NVIDIA A100 GPUs. During the outdoor pose estimation experiment, we compare LoFTR and MatchFormer at different data scales, using 8 NVIDIA A100 GPUs to keep the identical experimental conditions. We performed Image Matching, Homography Estimation, and InLoc Visual Localization experiments using the model trained with MatchFormer-large-LA on MegaDepth.

## 4.2. Indoor Pose Estimation

Indoor pose estimation is highly difficult due to wide areas devoid of textures, a high degree of self-similarity, scenes with complicated 3D geometry, and frequent perspective shifts. Faced with all these challenges, MatchFormer with interleaved self- and cross-attention modules still functions well as unfolded in the results.

Method	Pose estimation AUC			P
	@5°	@10°	@20°	
ORB [28]+GMS [2] <small>CVPR'17</small>	5.21	13.65	25.36	72.0
D2-Net [10]+NN <small>CVPR'19</small>	5.25	14.53	27.96	46.7
ContextDesc [22]+RT [21] <small>CVPR'19</small>	6.64	15.01	25.75	51.2
SP [8]+NN <small>CVPRW'18</small>	9.43	21.53	36.40	50.4
SP [8]+PointCN [43] <small>CVPR'18</small>	11.40	25.47	41.41	71.8
SP [8]+OANet [47] <small>ICCV'19</small>	11.76	26.90	43.85	74.0
SP [8]+SuperGlue [30] <small>CVPR'20</small>	16.16	33.81	51.84	84.4
LoFTR [33] <small>CVPR'21</small>	22.06	40.80	57.62	87.9
LoFTR [33]+QuadTree [36] <small>ICLR'22</small>	23.90	43.20	60.30	89.3
MatchFormer-lite-LA	20.42	39.23	56.82	87.7
MatchFormer-lite-SEA	22.89	42.68	60.66	89.2
MatchFormer-large-LA	20.22	38.23	55.55	87.8
MatchFormer-large-SEA	<b>24.31</b>	<b>43.90</b>	<b>61.41</b>	<b>89.5</b>

Table 2. **Indoor pose estimation on ScanNet.** The AUC of three different thresholds and the average matching precision (P) are evaluated.

**Metrics.** Following [30], we provide the area under the cumulative curve (AUC) of the pose error at three different thresholds ( $5^\circ$ ,  $10^\circ$ ,  $20^\circ$ ). The camera pose is recovered by using RANSAC. We report the matching precision (P), the probability of a true match if its epipolar is smaller than  $5 \times 10^{-4}$ .

**Quantitative Results.** As shown in Table 2, MatchFormer demonstrates exceptional performance on the low-texture indoor pose estimation task. The matching precision (P) of MatchFormer-large-SEA reaches the state-of-the-art level of 89.5%. Benefiting from the *extract-and-match* strategy, MatchFormer-large-SEA can bring +5.1% improvement over the *detector-based* SuperGlue, +1.6% over the *extract-to-match* LoFTR. Pose estimation AUC of MatchFormer is also significantly superior to *detector-based* SuperGlue. Both LoFTR and MatchFormer employ transformer-based techniques, and MatchFormer provides a more pronounced pose estima-

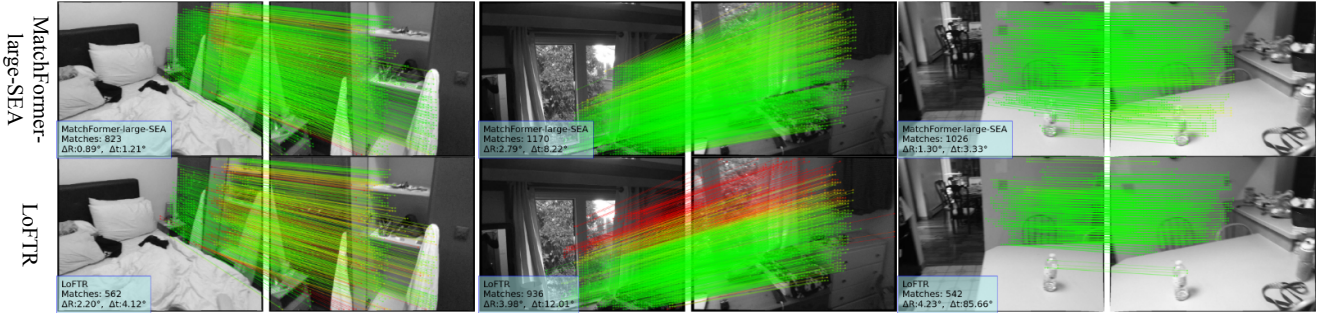


Figure 5. **Qualitative visualization** of MatchFormer and LoFTR [33]. MatchFormer achieves higher matching numbers and more correct matches in low-texture scenes.

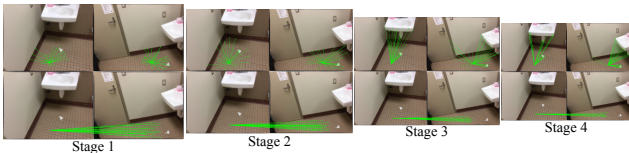


Figure 6. **Visualization of self- and cross-attention at multiple stages.** Cross-attention focuses on learning the similarity of image pairs and gradually refines the matching range, while self-attention focuses on detecting features of the image itself and enabling long-range dependencies.

tion AUC by boosting (+2.25%, +3.1%, +3.79%) at three thresholds of ( $5^\circ$ ,  $10^\circ$ ,  $20^\circ$ ). The LoFTR model is recently adapted by a complex decoder with QuadTree Attention [36]. However, MatchFormer maintains its lead (+0.41%, +0.70%, +1.11%) with the *extract-and-match* strategy. Additionally, compared to LoFTR, our lightweight MatchFormer-lite-SEA has only 45% GFLOPs, yet achieves a +1.3% precision gain and a 41% running speed boost. More details of the efficiency comparison will be presented in Table 7. Comparing SEA and LA, we found that the spatial scaling operation in SEA has benefits in handling low-texture features, thus it is more suited for indoor scenes and provides better results.

**Qualitative Results.** The visualizations of indoor matching results can be found in Fig. 5. In challenging feature-sparse indoor scenes, it can reliably capture global information to assure more matches and high matching accuracy. Therefore, the pose solved by matching prediction has a lower maximum angle error ( $\Delta R$ ) and translation error ( $\Delta t$ ). Due to the hierarchical transformer and interleaving-attention design, the receptive field of MatchFormer exceeds that of CNN-based methods. It confirms that applying cross-attention modules earlier for learning feature similarity robustifies low-texture indoor matching, which is in line with our *extract-and-match* pipeline.

**Self- and Cross-attention Visualization.** To further investigate the effectiveness of interleaving attention in MatchFormer, the features of self- and cross-attention modules in four stages are shown in Fig. 6. Self-attention connects ob-

scure points with surrounding points, while cross-attention learns relationship between points across images. Specifically, self-attention enables the query point to associate surrounding textural features in the shallow stage, and it enables the query point to connect to semantic features in the deep stage. As the model deepens, cross-attention will narrow the range of query points detected across images, rendering the matching much easier and more fine-grained. Finally, these four stages of features are blended, empowering the model to perform accurate feature matching in low-texture scenes.

### 4.3. Outdoor Pose Estimation

Outdoor pose estimation presents unique challenges compared to indoors. In particular, outdoor scenes have greater variations in lighting and occlusion. Still, MatchFormer achieves outstanding performance in outdoor scenes.

**Metrics.** We present the same AUC of the pose error as in the indoor pose estimation task. The matching precision pipolar distance threshold is  $1 \times 10^{-4}$ .

**Results.** As shown in Table 3, MatchFormer excels when facing outdoor scenes with considerable changes in illumination and viewpoint. For the pose estimation AUC at three different thresholds, MatchFormer noticeably surpasses the *detector-based* SuperGlue and DRC-Net, as well as the *extract-to-match* LoFTR. Our MatchFormer-lite-LA model also achieves great performance. It can deliver a higher matching precision (P) with 97.55%, despite being much lighter. Note that MatchFormer-large-SEA in Table 3 cannot be trained given the high resolution of outdoor images, since computations are only partially optimized by SEA (from  $O(N^2)$  to  $O(\frac{N^2}{R})$ ) and it will raise an out-of-memory issue. Nonetheless, our MatchFormer-large-LA model achieves consistent state-of-the-art performances on both metrics of AUC and P. To evaluate the robustness with less training data, we further compare MatchFormer-large-LA and LoFTR in different percentages of datasets in Table 3. The different sizes of training data are selected from the first  $x \in \{10, 30, 50, 70, 100\}$

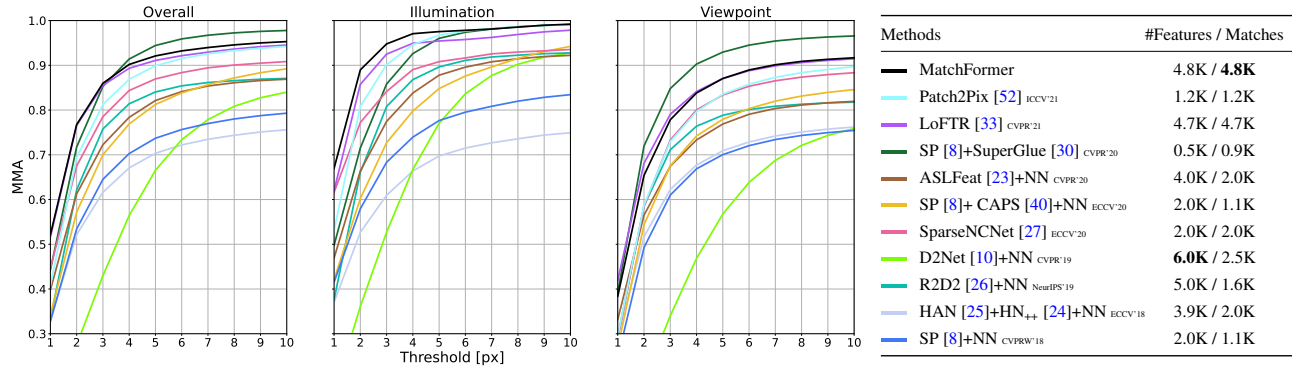


Figure 7. **Image matching on HPatches.** The mean matching accuracy (MMA) at thresholds from [1, 10] pixels, and the number of matches and features are reported.

Method	Data percent @5°	Pose estimation AUC			P
		@10°	@20°		
SP [8]+SuperGlue [30] <small>CVPR'20</small>	100%	42.18	61.16	75.95	–
DRC-Net [17] <small>NeurIPS'20</small>	100%	27.01	42.96	58.31	–
LoFTR [33] <small>CVPR'21</small>	100%	52.80	69.19	81.18	94.80
MatchFormer-lite-LA	100%	48.74	65.83	78.81	97.55
MatchFormer-lite-SEA	100%	48.97	66.12	79.07	97.52
MatchFormer-large-LA	100%	<b>52.91</b> (+0.11)	<b>69.74</b> (+0.55)	<b>82.00</b> (+0.82)	<b>97.56</b> (+2.76)
MatchFormer-large-SEA	100%	–	–	–	–
<b>Robustness with less training data:</b>					
LoFTR†	10%	38.81	54.53	67.04	83.64
MatchFormer†	10%	42.92 (+4.11)	58.33 (+3.80)	70.34 (+3.30)	85.08 (+1.44)
LoFTR†	30%	47.38	64.77	77.68	91.94
MatchFormer†	30%	49.53 (+2.15)	66.74 (+1.97)	79.43 (+1.75)	94.28 (+2.34)
LoFTR†	50%	48.68	65.49	77.62	92.54
MatchFormer†	50%	50.13 (+1.45)	66.71 (+1.22)	79.01 (+1.39)	94.89 (+2.35)
LoFTR†	70%	49.08	66.03	78.72	93.86
MatchFormer†	70%	51.22 (+2.14)	67.44 (+1.41)	79.73 (+1.01)	95.75 (+1.89)
LoFTR†	100%	50.85	67.56	79.96	95.18
MatchFormer†	100%	<b>53.28</b> (+2.43)	<b>69.74</b> (+2.18)	<b>81.83</b> (+1.87)	<b>96.59</b> (+1.41)

Table 3. **Outdoor pose estimation on MegaDepth.** † represents training on different percentages of datasets, which requires 8 GPUs for training.

percentages of the original dataset. With 100% percent data, MatchFormer† outperforms LoFTR† with improvements of (2.43%, 2.18%, 1.87%) at three thresholds of (5°, 10°, 20°), respectively, and a 1.41% improvement in precision. On other constrained datasets, MatchFormer has more clear benefits, and it has more promise in data-hungry real-world applications. Furthermore, our model achieves surprising results when equally limited to fewer resources (8 GPUs).

#### 4.4. Image Matching

**Metrics.** On the standard image matching task of HPatches sequences based on sequences with illumination or viewpoint change, we evaluate MatchFormer by detecting correspondences between pairs of input images. Following the experimental setup of Patch2Pix [52], we report the mean matching accuracy (MMA) at thresholds from [1, 10] pixels, and the number of matches and features.

**Results.** Fig. 7 illustrates the results for the experiments with illumination and viewpoint changes, along with the

MMA. Under varying illumination conditions, our method provides the best performance. On overall (the threshold  $\leq 3$  pixels), Matchformer performs optimally at precision levels. While other methods can only account for lighting changes or viewing angles changes, MatchFormer is reasonably compatible and maintains its functionality when the viewpoint changes. Thanks to the match-aware encoder, a larger number of features and matches, both 4.8K, are obtained. The results reveal the effectiveness of our *extract-and-match* strategy for image matching.

#### 4.5. Homography Estimation

**Metrics.** To evaluate how the matches contribute to the accuracy of the geometric relations estimation, we assess MatchFormer in the homography estimation on HPatches benchmark [1]. The proportion of accurately predicted homographies with an average corner error distance less than 1/3/5 pixels is reported.

**Results.** As shown in Table 4, MatchFormer achieves excellent performance on the HPatches benchmark in homography estimation. It reaches the best level in the face of illumination variations, delivering the accuracy of (0.75, 0.95, 0.98) at 1/3/5 pixel errors. Additionally, MatchFormer obtains highest number of matches with 4.8K. To make a more comprehensive comparison, we also executed experiments with varying dataset percentages in Table 4. Keeping the same experimental conditions, MatchFormer performed significantly better in homography experiments, and MatchFormer was relatively unaffected by the limited training data and had better generalization capabilities. MatchFormer trained with 30% data has a better performance in illumination variations. One reason is that the accuracy of the geometry relation estimation is related to accurate matches, as well as the distribution and number of matches [52]. These experiments sufficiently prove that our new *extract-and-match* pipeline has higher robustness than the *extract-to-match* one used in previous methods.

Method	Data percent	Overall	Illumination Accuracy (% , $\epsilon < 1/3/5$ px)	Viewpoint	#Matches
SP [8] <small>CVPRW'18</small>	100%	0.46/0.78/0.85	0.57/0.92/0.97	0.35/0.65/0.74	1.1K
D2Net [10] <small>CVPR'19</small>	100%	0.38/0.71/0.82	0.66/0.95/ <b>0.98</b>	0.12/0.49/0.67	2.5K
R2D2 [26] <small>NeurIPS'19</small>	100%	0.47/0.77/0.82	0.63/0.93/ <b>0.98</b>	0.32/0.64/0.70	1.6K
ASLFeat [23] <small>CVPR'20</small>	100%	0.48/0.81/0.88	0.62/0.94/ <b>0.98</b>	0.34/0.69/0.78	2.0K
SP [8] + SuperGlue [30] <small>CVPR'20</small>	100%	0.51/ <b>0.82/0.89</b>	0.60/0.92/ <b>0.98</b>	<b>0.42/0.71/0.81</b>	0.5K
SP [8] + CAPS [40] <small>ECCV'20</small>	100%	0.49/0.79/0.86	0.62/0.93/ <b>0.98</b>	0.36/0.65/0.75	1.1K
SIFT + CAPS [40] <small>ECCV'20</small>	100%	0.36/0.77/0.85	0.48/0.89/0.95	0.26/0.65/0.76	1.5K
SparseNCNet [27] <small>ECCV'20</small>	100%	0.36/0.65/0.76	0.62/0.92/0.97	0.13/0.40/0.58	2.0K
Patch2Pix [52] <small>CVPR'21</small>	100%	0.50/0.79/0.87	0.71/ <b>0.95/0.98</b>	0.30/0.64/0.76	1.3K
LoFTR [33] <small>CVPR'21</small>	100%	<b>0.55/0.81/0.86</b>	0.74/ <b>0.95/0.98</b>	0.38/0.69/0.76	4.7K
MatchFormer	100%	<b>0.55/0.81/0.87</b>	<b>0.75/0.95/0.98</b>	0.37/0.68/0.78	<b>4.8K</b>
<b>Robustness with less training data:</b>					
LoFTR†	10%	0.50/0.78/0.84	0.74/0.95/ <b>0.98</b>	0.28/0.63/0.71	3.6K
MatchFormer†	10%	0.50/0.78/0.84	0.72/0.93/0.97	0.30/0.64/0.71	4.0K
LoFTR†	30%	0.52/0.80/0.86	0.74/0.96/ <b>0.98</b>	0.32/0. <b>66</b> /0.74	4.1K
MatchFormer†	30%	<b>0.57/0.81/0.86</b>	<b>0.78/0.97/0.98</b>	<b>0.36/0.66</b> /0.74	4.4K
LoFTR†	50%	0.52/0.79/0.85	0.73/0.95/ <b>0.98</b>	0.32/0.65/0.73	4.1K
MatchFormer†	50%	0.54/0.78/0.85	0.75/0.95/ <b>0.98</b>	0.35/0.62/0.74	<b>4.5K</b>
LoFTR†	70%	0.52/0.79/0.85	0.74/0.94/ <b>0.98</b>	0.31/0.64/0.73	4.1K
MatchFormer†	70%	0.55/0.79/0.86	0.76/0.94/ <b>0.98</b>	0.35/0.64/0.75	<b>4.5K</b>
LoFTR†	100%	0.52/0.79/0.86	0.74/0.93/ <b>0.98</b>	0.32/0.65/0.74	4.2K
MatchFormer†	100%	0.54/0.79/ <b>0.87</b>	0.74/0.95/ <b>0.98</b>	<b>0.36/0.66/0.77</b>	<b>4.5K</b>

Table 4. **Homography estimation on HPatches.** † represents training on different percentages of datasets, which requires 8 GPUs.

#### 4.6. Visual Localization on InLoc

**Metrics.** A robust local feature matching method ensures accurate visual localization. To evaluate our local feature matching method MatchFormer, we test it on the InLoc [34] benchmark for visual localization. Referring to SuperGlue [30], we utilize MatchFormer as the feature matching step to complete the visual localization task along the localization pipeline HLoc [29].

**Results.** As shown in Table 5, on the InLoc benchmark for visual localization, MatchFormer reaches a level comparable to the current state of art methods SuperGlue and LoFTR. Interleaving attention in the MatchFormer backbone enables robust local feature matching in indoor scenes with large low-texture areas and repetitive structures.

#### 4.7. MatchFormer Structural Study

Performing the *extract-and-match* strategy in a pure transformer, the layout between self- and cross-attention co-existing inside each stage of MatchFormer is a critical point to achieve efficient and robust feature matching. To indicate the sweet spot to arrange different attention modules, a comprehensive variety of experiments is conducted.

**Ablation Study of Interleaving.** To verify the rationality of the model design, models in Table 6 are ablated according to different backbone structures, attention arrangements and patch embedding modules. Models are trained with 10% data of ScanNet. Such a setting is one for efficiency and

another is that the robustness between models is validated with less training data. By comparing 1) and 2), we establish that the transformer with self-attention significantly improves the matching precision (P, +5.2%) compared to utilizing the convolutional extractor, which shows the long-range dependency can robustify the local feature matching. While the structure in 2) contains only self-attention in between, the structure in 3) with cross-attention can bring a +3.1% performance gain, which demonstrates the benefits of leaning feature similarity inside a transformer. The sequential structure of 4) and 5) applies pure self-attention in the early stages and pure cross-attention in the later stages, while our interleaving structure of 6) and 7) applies mix self-/cross-attention in each stage. The comparison between 4) and 5) indicates that the proposed PosPE is capable of completing the fixed position encoding and it comes with a +0.8% gain. Between 5) and 7), in contrast to the sequential combination in 5), our interleaving combination in 7) improves the overall performance, which adaptively inserts self-/cross-attention in multi-scale stages, and it is in line with our statement about the *extract-and-match* strategy in transformers. Our PosPE in experiment 7) can enhance the accuracy by +0.8% compared with standard PE (StdPE) used in 6), demonstrating that PosPE is more robust. Our interleaving model in 7) surpasses LoFTR by a large margin (+4.1% @ P), indicating that MatchFormer is more robust, not only in low-texture indoor scenes, but also with less training data.



Method	Localized Queries (% , 0.25m/0.5m/1.0m, 10°)	
	DUC1	DUC2
SP [8] + NN <small>CVPR'18</small>	40.4 / 58.1 / 69.7	42.0 / 58.8 / 69.5
D2Net [10] + NN <small>CVPR'19</small>	38.4 / 56.1 / 71.2	37.4 / 55.0 / 64.9
R2D2 [26] + NN <small>SeasPS'19</small>	36.4 / 57.6 / 74.2	45.0 / 60.3 / 67.9
SP [8] + SuperGlue [30] <small>CVPR'20</small>	<b>49.0</b> / 68.7 / 80.8	53.4 / <b>77.1</b> / 82.4
SP [8] + CAPS [40] + NN <small>ECCV'20</small>	40.9 / 60.6 / 72.7	43.5 / 58.8 / 68.7
SIFT + CAPS [40] + NN <small>ECCV'20</small>	38.4 / 56.6 / 70.7	35.1 / 48.9 / 58.8
SparseNCNet [27] <small>ECCV'20</small>	41.9 / 62.1 / 72.7	35.1 / 48.1 / 55.0
Patch2Pix [52] <small>CVPR'21</small>	44.4 / 66.7 / 78.3	49.6 / 64.9 / 72.5
LoFTR-OT [33] <small>CVPR'21</small>	47.5 / 72.2 / 84.8	54.2 / 74.8 / <b>85.5</b>
MatchFormer	46.5 / <b>73.2</b> / <b>85.9</b>	<b>55.7</b> / 71.8 / 81.7

Table 5. **Visual localization on InLoc [34]**. We report the percentage of correctly localized queries under specific error thresholds, following the HLOC [29] pipeline.

Method	Self Cross PosPE StdPE	Pose estimation AUC			P	
		@5°	@10°	@20°		
LoFTR [33] <small>CVPR'21</small>		15.47	31.72	48.63	82.6	
1) Convolution		7.36	18.17	32.21	76.1	
2) Self-only	✓	9.48	22.68	38.10	81.3	
3) Cross-only	✓	13.88	29.98	46.89	84.4	
4) Sequential	✓ ✓	14.75	31.03	48.27	85.0	
5) Sequential	✓ ✓ ✓	17.32	34.85	52.71	85.8	
6) Interleaving	✓ ✓ ✓	✓	16.53	34.63	52.31	85.9
7) Interleaving	✓ ✓ ✓	<b>18.01</b>	<b>35.87</b>	<b>53.46</b>	<b>86.7</b>	

Table 6. **Ablation study** with different structures, arrangements and PEs.

Method	#Params	GFLOPs	Runtime	P
LoFTR [33] <small>CVPR'21</small>	<b>11</b>	307	202	87.9
LoFTR [33]+QuadTree [36] <small>ICLR'22</small>	13	393	234	89.3
MatchFormer-lite-LA	22	<b>97</b>	140	87.7
MatchFormer-large-LA	22	389	246	87.8
MatchFormer-lite-SEA	23	140	<b>118</b>	89.2
MatchFormer-large-SEA	23	414	390	<b>89.5</b>

Table 7. **Efficiency analysis**. Runtime in *ms*, GFLOPs @ 640×480.

**Feature Maps Comparison.** As shown in Fig. 8, we visualize the feature maps of the ablation experiment 2) and 7) of Table 6. In both shallow and deep layers, the interleaving attention structure of experiment 7) enables MatchFormer to capture dense features and learn feature similarities, such as the paired regions highlighted in yellow. The model with only self-attention tends to extract features in each individual image and neglects the matching-aware features across images, *i.e.*, without cross-attention weights. As a result, the self-attention model without cross-attention model will be incapable of matching local features when the image features are sparse (*i.e.*, low-texture scenes).

**Runtime and Efficiency Analysis.** Aside from verifying the effectiveness of arranging self- and cross-attention in an interleaving manner, MatchFormer is still supposed to be computationally efficient. The comparisons of efficiency results including the number of parameters ( $M$ ), GFLOPs, and runtime (*ms*) are detailed in Table 7. Based on a 3080Ti GPU, MatchFormer is compared against the pre-

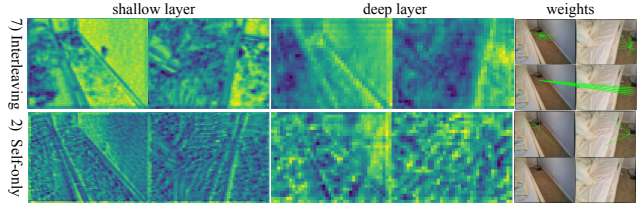


Figure 8. **Feature maps comparison** between interleaving and self-only attention in shallow and deep layers (from the last layer of the stage-2 and stage-3, respectively).

vious transformer-based LoFTR. We quantify the average runtime it takes for MatchFormer to complete a single image pair on the ScanNet test set, which includes 1,500 pairs of images in the resolution of 640×480. MatchFormer-lite-SEA is clearly much faster, speeding up the matching process by 41%, although a higher number of parameters is required. Additionally, we compute the GFLOPs of the two approaches to determine their computing costs and storage demands. The GFLOPs of MatchFormer-lite-SEA are only 45% of those of LoFTR. Yet, our model achieves a +1.3% precision gain. Thanks to interleaving self- and cross-attention in between, our lite and large MatchFormers achieve state-of-the-art performances with respect to previous methods on various tasks.

## 5. Conclusions

Rethinking local feature matching from a novel *extract-and-match* perspective with transformers, we propose the MatchFormer framework equipped with a matching-aware encoder by interleaving self- and cross-attention for performing feature extraction and feature similarity learning synchronously. MatchFormer circumvents involving a complex decoder as used in the *extract-to-match* methods and adopts a lightweight FPN-like decoder to fuse multi-scale features. Experiments show that MatchFormer achieves state-of-the-art performances in indoor and outdoor pose estimation on the ScanNet and MegaDepth benchmarks, and in both homography estimation and image matching on the HPatches benchmark, as well as in visual localization on the InLoc benchmark.

## Acknowledgement

This work was supported in part by the Federal Ministry of Labor and Social Affairs (BMAS) through the AccessibleMaps project under Grant 01KM151112, in part by the University of Excellence through the “KIT Future Fields” project, in part by the Helmholtz Association Initiative and Networking Fund on the HAICORE@KIT partition, and in part by Hangzhou SurImage Technology Company Ltd.

## References

- [1] Vassileios Balntas, Karel Lenc, Andrea Vedaldi, and Krystian Mikolajczyk. HPatches: A benchmark and evaluation of handcrafted and learned local descriptors. In *CVPR*, 2017. 2, 7
- [2] JiaWang Bian, Wen-Yan Lin, Yasuyuki Matsushita, Sai-Kit Yeung, Tan-Dat Nguyen, and Ming-Ming Cheng. GMS: Grid-based motion statistics for fast, ultra-robust feature correspondence. In *CVPR*, 2017. 5
- [3] Nicolas Carion, Francisco Massa, Gabriel Synnaeve, Nicolas Usunier, Alexander Kirillov, and Sergey Zagoruyko. End-to-end object detection with transformers. In *ECCV*, 2020. 1, 3
- [4] Hao Chen, Weijian Hu, Kailun Yang, Jian Bai, and Kaiwei Wang. Panoramic annular SLAM with loop closure and global optimization. *Applied Optics*, 2021. 1
- [5] Liang-Chieh Chen, George Papandreou, Iasonas Kokkinos, Kevin Murphy, and Alan L. Yuille. DeepLab: Semantic image segmentation with deep convolutional nets, atrous convolution, and fully connected CRFs. *IEEE Transactions on Pattern Analysis and Machine Intelligence*, 2018. 3
- [6] Ruiqi Cheng, Kaiwei Wang, Longqing Lin, and Kailun Yang. Visual localization of key positions for visually impaired people. In *ICPR*, 2018. 2
- [7] Angela Dai, Angel X. Chang, Manolis Savva, Maciej Halber, Thomas Funkhouser, and Matthias Nießner. ScanNet: Richly-annotated 3D reconstructions of indoor scenes. In *CVPR*, 2017. 2, 4
- [8] Daniel DeTone, Tomasz Malisiewicz, and Andrew Rabinovich. SuperPoint: Self-supervised interest point detection and description. In *CVPRW*, 2018. 5, 7, 8, 9
- [9] Alexey Dosovitskiy, Lucas Beyer, Alexander Kolesnikov, Dirk Weissenborn, Xiaohua Zhai, Thomas Unterthiner, Mostafa Dehghani, Matthias Minderer, Georg Heigold, Sylvain Gelly, Jakob Uszkoreit, and Neil Houlsby. An image is worth 16x16 words: Transformers for image recognition at scale. In *ICLR*, 2021. 1, 3, 4
- [10] Mihai Dusmanu, Ignacio Rocco, Tomas Pajdla, Marc Pollefeys, Josef Sivic, Akihiko Torii, and Torsten Sattler. D2-net: A trainable CNN for joint detection and description of local features. *CVPR*, 2019. 1, 2, 3, 5, 7, 8, 9
- [11] Jakob Engel, Vladlen Koltun, and Daniel Cremers. Direct sparse odometry. *IEEE Transactions on Pattern Analysis and Machine Intelligence*, 2018. 1
- [12] Patrick Esser, Robin Rombach, and Bjorn Ommer. Taming transformers for high-resolution image synthesis. In *CVPR*, 2021. 3
- [13] Yicheng Fang, Kaiwei Wang, Ruiqi Cheng, and Kailun Yang. CFVL: A coarse-to-fine vehicle localizer with omnidirectional perception across severe appearance variations. In *IV*, 2020. 2
- [14] Wei Jiang, Eduard Trulls, Jan Hosang, Andrea Tagliasacchi, and Kwang Moo Yi. COTR: Correspondence transformer for matching across images. *arXiv preprint arXiv:2103.14167*, 2021. 1, 3, 4
- [15] Diederik P. Kingma and Jimmy Ba. Adam: A method for stochastic optimization. In *ICLR*, 2015. 5
- [16] Shiwei Li, Lu Yuan, Jian Sun, and Long Quan. Dual-feature warping-based motion model estimation. In *ICCV*, 2015. 1
- [17] Xinghui Li, Kai Han, Shuda Li, and Victor Prisacariu. Dual-resolution correspondence networks. *NeurIPS*, 2020. 2, 3, 4, 7
- [18] Zhengqi Li and Noah Snavely. MegaDepth: Learning single-view depth prediction from internet photos. In *CVPR*, 2018. 2, 5
- [19] Philipp Lindenberger, Paul-Edouard Sarlin, Viktor Larsson, and Marc Pollefeys. Pixel-perfect structure-from-motion with featuremetric refinement. In *ICCV*, 2021. 1
- [20] Ze Liu, Yutong Lin, Yue Cao, Han Hu, Yixuan Wei, Zheng Zhang, Stephen Lin, and Baining Guo. Swin transformer: Hierarchical vision transformer using shifted windows. In *ICCV*, 2021. 3
- [21] David G. Lowe. Distinctive image features from scale-invariant keypoints. *International Journal of Computer Vision*, 2004. 5
- [22] Zixin Luo, Tianwei Shen, Lei Zhou, Jiahui Zhang, Yao Yao, Shiwei Li, Tian Fang, and Long Quan. ContextDesc: Local descriptor augmentation with cross-modality context. In *CVPR*, 2019. 1, 5
- [23] Zixin Luo, Lei Zhou, Xuyang Bai, Hongkai Chen, Jiahui Zhang, Yao Yao, Shiwei Li, Tian Fang, and Long Quan. ASLFeat: Learning local features of accurate shape and localization. In *CVPR*, 2020. 2, 7, 8
- [24] Anastasiia Mishchuk, Dmytro Mishkin, Filip Radenovic, and Jiri Matas. Working hard to know your neighbor’s margins: Local descriptor learning loss. *NeurIPS*, 2017. 7
- [25] Dmytro Mishkin, Filip Radenovic, and Jiri Matas. Repeatability is not enough: Learning affine regions via discriminability. In *ECCV*, 2018. 7
- [26] Jerome Revaud, Cesar De Souza, Martin Humenberger, and Philippe Weinzaepfel. R2D2: Reliable and

- repeatable detector and descriptor. In *NeurIPS*, 2019. 1, 2, 3, 7, 8, 9
- [27] Ignacio Rocco, Relja Arandjelović, and Josef Sivic. Efficient neighbourhood consensus networks via sub-manifold sparse convolutions. In *ECCV*, 2020. 7, 8, 9
- [28] Ethan Rublee, Vincent Rabaud, Kurt Konolige, and Gary Bradski. ORB: An efficient alternative to SIFT or SURF. In *ICCV*, 2011. 1, 5
- [29] Paul-Edouard Sarlin, Cesar Cadena, Roland Siegwart, and Marcin Dymczyk. From coarse to fine: Robust hierarchical localization at large scale. In *CVPR*, 2019. 1, 8, 9
- [30] Paul-Edouard Sarlin, Daniel DeTone, Tomasz Malisiewicz, and Andrew Rabinovich. SuperGlue: Learning feature matching with graph neural networks. In *CVPR*, 2020. 1, 2, 3, 5, 7, 8, 9
- [31] Johannes L. Schonberger and Jan-Michael Frahm. Structure-from-motion revisited. In *CVPR*, 2016. 1, 5
- [32] Zhuoran Shen, Mingyuan Zhang, Haiyu Zhao, Shuai Yi, and Hongsheng Li. Efficient attention: Attention with linear complexities. In *WACV*, 2021. 2, 4
- [33] Jiaming Sun, Zehong Shen, Yuang Wang, Hujun Bao, and Xiaowei Zhou. LoFTR: Detector-free local feature matching with transformers. In *CVPR*, 2021. 1, 2, 3, 5, 6, 7, 8, 9
- [34] Hajime Taira, Masatoshi Okutomi, Torsten Sattler, Mircea Cimpoi, Marc Pollefeys, Josef Sivic, Tomas Pajdla, and Akihiko Torii. InLoc: Indoor visual localization with dense matching and view synthesis. In *CVPR*, 2018. 1, 2, 8, 9
- [35] Shitao Tang, Chengzhou Tang, Rui Huang, Siyu Zhu, and Ping Tan. Learning camera localization via dense scene matching. In *CVPR*, 2021. 3
- [36] Shitao Tang, Jiahui Zhang, Siyu Zhu, and Ping Tan. Quadtree attention for vision transformers. *ICLR*, 2022. 2, 3, 5, 6, 9
- [37] Hugo Touvron, Matthieu Cord, Matthijs Douze, Francisco Massa, Alexandre Sablayrolles, and Hervé Jégou. Training data-efficient image transformers & distillation through attention. In *ICML*, 2021. 3
- [38] Ashish Vaswani, Noam Shazeer, Niki Parmar, Jakob Uszkoreit, Llion Jones, Aidan N. Gomez, Łukasz Kaiser, and Illia Polosukhin. Attention is all you need. In *NeurIPS*, 2017. 1, 3
- [39] Huiyu Wang, Yukun Zhu, Bradley Green, Hartwig Adam, Alan Yuille, and Liang-Chieh Chen. Axial-DeepLab: Stand-alone axial-attention for panoptic segmentation. In *ECCV*, 2020. 1
- [40] Qianqian Wang, Xiaowei Zhou, Bharath Hariharan, and Noah Snavely. Learning feature descriptors using camera pose supervision. In *ECCV*, 2020. 1, 2, 7, 8, 9
- [41] Wenhai Wang, Enze Xie, Xiang Li, Deng-Ping Fan, Kaitao Song, Ding Liang, Tong Lu, Ping Luo, and Ling Shao. Pyramid vision transformer: A versatile backbone for dense prediction without convolutions. In *ICCV*, 2021. 2, 3, 4
- [42] Enze Xie, Wenhai Wang, Zhiding Yu, Anima Anandkumar, Jose M. Alvarez, and Ping Luo. SegFormer: Simple and efficient design for semantic segmentation with transformers. In *NeurIPS*, 2021. 3, 4
- [43] Kwang Moo Yi, Eduard Trulls, Yuki Ono, Vincent Lepetit, Mathieu Salzmann, and Pascal Fua. Learning to find good correspondences. In *CVPR*, 2018. 5
- [44] Sungho Yoon and Ayoung Kim. Line as a visual sentence: Context-aware line descriptor for visual localization. *IEEE Robotics and Automation Letters*, 2021. 1
- [45] Fisher Yu and Vladlen Koltun. Multi-scale context aggregation by dilated convolutions. *ICLR*, 2016. 3
- [46] Li Yuan, Yunpeng Chen, Tao Wang, Weihao Yu, Yujun Shi, Francis E. H. Tay, Jiashi Feng, and Shuicheng Yan. Tokens-to-token ViT: Training vision transformers from scratch on ImageNet. In *ICCV*, 2021. 3, 4
- [47] Jiahui Zhang, Dawei Sun, Zixin Luo, Anbang Yao, Lei Zhou, Tianwei Shen, Yurong Chen, Long Quan, and Hongen Liao. Learning two-view correspondences and geometry using order-aware network. In *ICCV*, 2019. 5
- [48] Jiaming Zhang, Kailun Yang, Angela Constantinescu, Kunyu Peng, Karin Müller, and Rainer Stiefelhagen. Trans4Trans: Efficient transformer for transparent object segmentation to help visually impaired people navigate in the real world. In *ICCVW*, 2021. 3
- [49] Zhaoyang Zhang, Yitong Jiang, Jun Jiang, Xiaogang Wang, Ping Luo, and Jinwei Gu. STAR: A structure-aware lightweight transformer for real-time image enhancement. In *ICCV*, 2021. 3
- [50] Sixiao Zheng, Jiachen Lu, Hengshuang Zhao, Xiatian Zhu, Zekun Luo, Yabiao Wang, Yanwei Fu, Jianfeng Feng, Tao Xiang, Philip H. S. Torr, and Li Zhang. Rethinking semantic segmentation from a sequence-to-sequence perspective with transformers. In *CVPR*, 2021. 1, 3
- [51] Guo Zhong and Chi-Man Pun. Subspace clustering by simultaneously feature selection and similarity learning. *Knowledge-Based Systems*, 2020. 2

- [52] Qunjie Zhou, Torsten Sattler, and Laura Leal-Taixe. Patch2Pix: Epipolar-guided pixel-level correspondences. In *CVPR*, 2021. 7, 8, 9
- [53] Zhili Zhou, Q. M. Jonathan Wu, Shaohua Wan, Wendi Sun, and Xingming Sun. Integrating SIFT and CNN feature matching for partial-duplicate image detection. *IEEE Transactions on Emerging Topics in Computational Intelligence*, 2020. 1
- [54] Xizhou Zhu, Weijie Su, Lewei Lu, Bin Li, Xiang Wang, and Jifeng Dai. Deformable DETR: Deformable transformers for end-to-end object detection. In *ICLR*, 2021. 3